

0584–8547(94)00138–3

## Fundamental studies on pneumatic generation and aerosol transport in atomic spectrometry: effect of mineral acids on emission intensity in inductively coupled plasma atomic emission spectrometry\*

A. CANALS,† V. HERNANDIS, J. L. TODOLÍ

Universidad de Alicante, Departamento de Química Analítica, 03071, Alicante, Spain

and

R. F. BROWNER

School of Chemistry and Biochemistry, Georgia Institute of Technology, Atlanta GA 30332, U.S.A.

(Received 21 March 1994; accepted 22 October 1994)

**Abstract**—The mechanism of the mineral acid interference has been studied in ICP–AES. For this study five mineral acids have been evaluated (HCl, HNO<sub>3</sub>, HClO<sub>4</sub>, H<sub>2</sub>SO<sub>4</sub> and H<sub>3</sub>PO<sub>4</sub>) in four concentrations (0, 0.5, 5 and 30%). In order to investigate this interference emission signal, sample uptake rate, primary and tertiary drop size distributions, total analyte transport rate and excitation temperature have been measured. From the results obtained, it seems that this interference is contributed by a reduction of the analyte transport rate and, also, by a decrease in the plasma temperature. The degree of the contribution to the interference of each one of these causes depends on the type of acid and sample uptake mode. The physical properties of the acid solutions are in the origin of the interference. These physical properties modify the sample uptake rate and/or the primary drop size distribution of the aerosols. The acids evaluated can be classified in two groups. The first group would consist of HCl, HNO<sub>3</sub> and HClO<sub>4</sub>, and the second one of H<sub>2</sub>SO<sub>4</sub> and H<sub>3</sub>PO<sub>4</sub>. In natural uptake mode the interference is mainly due to changes in sample uptake rate, and in controlled uptake mode to changes in primary drop size distribution of the aerosols. In both sample uptake modes a density-effect may appear on increasing acid concentration. All these factors tend to decrease the analyte transport rate and, hence, the emission signal. Finally, a cooling effect of the plasma due to a higher load of acids is superimposed to these causes.

We think that from this study the mineral acid interference in ICP–AES, with pneumatic nebulization, should be better understood.

### INTRODUCTION

SOLUTION nebulization is the most common way of sample introduction in atomic spectrometry. In the nebulization process an aerosol is generated that is then transported through the nebulization chamber to atomizer. During its transport significant amounts of aerosol are lost (i.e., 85–95% in FAAS and 97–99% in ICP–AES). Pneumatic and ultrasonic nebulization are the most common ways of aerosol generation in atomic spectrometry. Excellent reviews of these subjects have been written by SNEDDON [1], BROWNER [2] and GUSTAVSSON [3].

In contrast with the high effort that has been done in the study on the influence of the easily ionized elements in plasma emission spectrometry, little has been done on the effects of the mineral acids, and the results appear to be contradictory in many instances. However, it should be borne in mind that the acids are widely used for sample digestion and preservation [4–9]. It has been frequently reported that increasing acid concentrations give rise to a decrease in emission intensity [10, 11]. This interfering effect has been described both in natural and in controlled uptake modes, although the degree of interference is lower in the latter. The interference has been mainly studied with pneumatic nebulizers (i.e., concentric and cross-flow), but depressive

\* This paper was published in the Special Issue on Sample Introduction in Atomic Spectrometry.

† Author to whom correspondence should be sent.

effects have also been reported with thermospray [12] and ultrasonic [11, 13, 14] nebulizers. This interference effect has been attributed to the following causes [15]:

1. Changes in the sample uptake rate due to changes in physical properties of the solution, mainly viscosity [16].
2. Changes in aerosol drop size distribution due also to changes in the physical properties of the solution, mainly surface tension and viscosity [17, 18].
3. Changes in analyte transport rate due to causes 1 and 2 [17, 19–25].
4. Changes in the plasma excitation conditions due to the increased energy consumption for acid atomization [13, 15, 26–28].

The contributions to the interference of the mineral acids in atomic spectrometry can be classified into two clearly separated groups that are physically different: (a) those arising from the aerosol generation and transport system (i.e., nebulizer/spray chamber); and (b) those produced in the plasma itself. Recently, FERNÁNDEZ *et al.* [15] have classified the ICP instrumental conditions into two main groups, according to the value of the intensity ratio Mg II/Mg I. When this ratio is higher than 8 (condition type 1) the interference is mainly attributed to changes in the generation and transport of the aerosol, while this ratio is lower than 4 (condition type 3) the interference is also contributed by changes in the plasma itself. Type 1 conditions, which could be called “hot conditions”, imply high incident powers and low carrier/nebulizing gas flows, whereas type 3 conditions, “cold conditions”, imply low incident powers and high carrier/nebulizing gas flows. Thus, in principle, the two types of contribution could be studied separately by making a judicious choice of the instrumental conditions. Moreover, some previously published results can be easier to explain to the light of this classification of the instrumental conditions. So, GREENFIELD *et al.* [16] were clearly working under conditions of the type 1 (high power generator) and, hence, are allowed to think that the interference, in this case, was mainly contributed by the processes of aerosol generation and transport, so that it could be compensated for by means of the ratio relative emission/natural uptake rate,  $I_{\text{rel}}/Q_n$ .

Several systems have been proposed to correct this interference in atomic spectrometry [23, 24, 29–32], the most common being matrix matching, internal reference and standard addition. Some other correction methods have also been used: normalizing the signal with respect to the sample uptake rate [16]; normalizing the signal with respect to the analyte transport rate [20]; using mathematical methods [33]; normalizing the signal with respect to the energy dispersed, through Fraunhofer diffraction, by the tertiary aerosol [17]; increasing the incident power by an amount of 20–30 W, when using ionic lines [34].

To our knowledge experimental data have been published giving support, in a more or less concluding way, to causes 1 and 4, but not clearly to cause 3 and not at all to cause 2.

With respect to cause 3, FARINO *et al.* [20] measured the analyte transport efficiency, in natural uptake mode, for an acid concentration of 30% obtaining 0.52% and 0.71% for solutions of  $\text{H}_2\text{SO}_4$  and  $\text{H}_3\text{PO}_4$ , respectively. SHEN and CHEN [24] reported experimental data of transport for five analytes (i.e., Mn, Fe, Cr, Cu and Ni) in controlled uptake mode with  $\text{H}_3\text{PO}_4$  solutions (0 and 1.5%, w/v). They concluded that, for a given acid concentration, the mass of analyte transported were the same for all the analytes, and that this mass was higher for the solutions with no acid (i.e., without acid: 2.3–2.5  $\mu\text{g}$ ; with acid: 1.0–1.2  $\mu\text{g}$ ). KITAGAWA and KIKUCHI [17] measured the drop size distributions of the aerosols coming from  $\text{H}_2\text{SO}_4$  solutions (0–5 M). These aerosols were generated with a common regulable nebulizer used in FAAS and measured before entering the burner. These authors observed a decrease in the liquid volume of the “tertiary” aerosol on increasing acid concentration. More recently, MARICHY *et al.* [25] have measured the transport of acid and solvent at the exit of the spray chamber, concluding that there is a 50% reduction in the acid concentration, both for HCl and  $\text{HClO}_4$  solutions at 0.001% w/v, and only a slight increase in the amount of aerosol (solvent) as the acid concentration increases. The authors speculate about the possibility of an aerosol ionic redistribution (AIR) to explain not only this

Table 1. Instrumental conditions in ICP–AES

	Instrument	
	Perkin-Elmer	Baird
Incident power (kW)	1.25	0.8
Reflected power (W)	< 5	< 5
Integration time (sec)	1	0.2
Outer gas flow (l/min)	13.5	8.5
Intermediate gas flow (l/min)	0.9	1.0
Nebulizing/carrier gas flow (l/min)	0.8	0.8
Observation height (mm ALC)	10	7
Nebulizer	Meinhard TR-30-A3	
Spray chamber	Scott type	
Torch	Fassel type (1.5 mm id)	
Sample uptake rate	Variable*	

\* In natural mode the uptake rate was variable, while in controlled mode was fixed at 1 ml/min.

behaviour, but also the anomalous behaviour of the signal. CLIFFORD *et al.* [18] characterized the desolvated aerosols generated from  $\text{HNO}_3$  and  $\text{H}_2\text{SO}_4$  solutions (1–10%, v/v) by means of an ultrasonic nebulizer, and they concluded that the volume flux ( $F$ ) of aerosol increased as acid was increased.

Few papers supply experimental results supporting interference cause 2, and even those just report about the tertiary aerosol. KITAGAWA and KIKUCHI [17], under the conditions indicated above, found an increased dispersion of the drop sizes on increasing acid concentration. MARICHY *et al.* [25] did not find noticeable changes in the drop size distributions of the aerosols leaving the spray chamber when working with HCl solutions from 0 to 1%. CLIFFORD *et al.* [18], under the conditions indicated above, measured the Sauter mean diameter,  $D_{3,2}$ , of the desolvated aerosols. They found that  $D_{3,2}$  values increased on an increasing acid concentration, and that these values were higher for  $\text{H}_2\text{SO}_4$  than for  $\text{HNO}_3$ . From all these results one can conclude that there are no published data about drop size distributions of the primary aerosols in connection with the acid interference, and that only partial and sometimes contradictory data exist about tertiary aerosols and analyte transport. Thus, a systematic study is needed that takes into account the aerosol generation and transport processes as well as those taking place in the plasma itself in order to clarify the action of mineral acids in atomic spectrometry. Therefore, the present work is aimed to make a thorough study of the interference of the mineral acids, both in natural and controlled uptake modes, mainly from the point of view of the drop size distributions (primary and tertiary) and the transport of analyte. In this respect, the results outlined in this paper try to represent a comprehensive report on the fundamentals of the acidic aerosol generation and transport with pneumatic nebulizers.

## EXPERIMENTAL

A Baird 2070 Plasma Spectrometer has been used for temperature measurements. The emission intensity measurements have been carried out with a Perkin-Elmer ICP-5500 Plasma Spectrometer. Table 1 shows the instrumental conditions used with both instruments. The nebulizing/carrier gas flow was controlled by means of a mass flow controller. A peristaltic pump was used for the control of sample uptake rate when required.

The mineral acids studied were HCl,  $\text{HNO}_3$ ,  $\text{HClO}_4$ ,  $\text{H}_2\text{SO}_4$  and  $\text{H}_3\text{PO}_4$  in concentrations of 0, 0.5, 5 and 30% (w/w).

Drop size distributions for the primary and tertiary aerosols were measured with an instrument based on Fraunhofer diffraction of a laser beam (Malvern Inst., Mod. 2600c), using a lens of 63 mm focal length which allows drop size measurements in the range from 1.2 to 118  $\mu\text{m}$ . The calculation of the drop size distributions has been done with the software SB.0C, using a model-

Table 2. Elements and lines studied

Element	Line (nm)	E.P. (eV)	I.P. (eV)
Mn I	279.48	4.44	—
Mn II	257.61	4.81	7.43
Zn I	213.85	5.80	—
Zn II	202.54	6.13	9.39
Ca I	422.70	2.93	—
Ca II	393.30	3.12	6.14

independent algorithm. Primary aerosols were measured at 7.0 mm from the nebulizer tip, and the tertiary at 6.0 mm from the end of a conical glass-piece, specially designed to confine all the tertiary aerosol within the width of the laser beam, adapted to the exit of the spray chamber.

Solutions containing 50 µg/ml of Ca, Mn and Zn were used for emission intensity and drop size distribution measurements.

Total analyte transport rate,  $W_{\text{tot}}$ , was measured by collecting the tertiary aerosol in a glass fiber filter (Gelman, A/E Type, 47 mm diameter, 0.3 µm pore size) placed in acid resistant holder (NALGENE™) [20]. The filter holder was mounted vertically in line above the exit port of the spray chamber. Tertiary aerosols, carried by an external and extra air stream of 10–15 l/min, were collected during 20 minutes. After that, the analytes were extracted from the filter with hot water containing 5 ml of HNO<sub>3</sub> (1 M) during 40 minutes. Then the solutions were filtered and made up to 100 ml with deionized water. Finally, the analyte concentrations were determined by ICP–AES. The final acid concentration in these solutions (acid used for the extraction plus acid in the tertiary aerosol) is well below the lowest acid concentration required for the interference to be detectable. In these experiments multielemental solutions of Ca, Mn and Zn (1000 µg/ml each) were used, except in the H<sub>2</sub>SO<sub>4</sub> series because of the precipitation of CaSO<sub>4</sub>. The transport of Ca was not measured in any case since the filters contained and leached this element.

The study of the effect of solvent load on plasma excitation temperatures was performed, with a set of five iron lines, by using the linear Boltzmann plot method [35, 36].

The elements and lines used in this study have been chosen in such a way that they cover a wide range of energies (ionization and excitation) (Table 2).

## RESULTS AND DISCUSSION

### A. Emission intensity vs. acid concentration

YOSHIMURA *et al.* [28] stated that the degree of the interference depends on the energy and type (i.e., ionic or atomic) of the emission line employed, being the degree of the interference increasing on increasing the energy of the line. On the contrary, BUDIC and HUDNIK [34] and GREENFIELD *et al.* [16] did not observe any dependence of the interference degree on the type or energy of the line. These contradictory results could be explained in the light of the work by FERNÁNDEZ *et al.* [15], discussed previously. Thus, while BUDIC and HUDNIK, GREENFIELD *et al.* worked under conditions of the type 1, YOSHIMURA *et al.* were probably working under conditions of the type 3. According to FERNÁNDEZ *et al.* [15] neither electronic density,  $n_e$ , nor excitation temperature,  $T_{\text{exc}}$ , vary on increasing the acid concentration, when working under conditions of the type 1, so as the interference can be assigned just to the sample introduction system. Under conditions of the type 3,  $n_e$  decreases and  $T_{\text{exc}}$  does not vary on increasing acid concentration, so the interference is stronger for all the lines, mainly for the ionic ones. The observation that the acid concentration has no effect on  $T_{\text{exc}}$  under condition 3 differs from those obtained by other workers [27, 28]. So, a clear contradiction is observed in the data published about the degree of interference and its dependence on the type and energy of the emission line. In this point it must be indicated that sometimes it would be difficult to compare data from different workers because different conditions were used (i.e., incident power, sample uptake mode, acid type and concentration, type and energy of emission line, element

concentration, method to obtain the  $T_{\text{exc}}$ , etc.). Thus, in a thorough study devoted to the fundamentals of the mineral acid interference in plasma emission, firstly the degree of interference is needed to study with the five most common acids, in different concentrations, and with emission lines that cover a wide total excitation energy, both in natural and controlled uptake modes.

**A.1. Natural uptake mode.** Figure 1 shows the relative emission intensities obtained in natural uptake mode (1a–c) and controlled uptake mode (1d) for all the elements under study vs. acid concentration, for each of the acids.

First of all, from Figs 1a–c it appears that the emission intensity decreases on increasing acid concentration. In addition, two clearly different acid-type behaviours are noted. For HCl, HNO<sub>3</sub> and HClO<sub>4</sub> the relative signal decrease reaches 50–60% for the highest acid concentration (30%, w/w), while for H<sub>2</sub>SO<sub>4</sub> and H<sub>3</sub>PO<sub>4</sub> the signal decrease reaches 70–80% (Fig. 1c). It also appears that the signal decrease does not seem to be related to the type and energy of the emission line (Figs 1a–c). These observations have been published previously [16, 21, 34].

**A.2. Controlled uptake mode.** Usually, it has been indicated that using a peristaltic pump to control the sample uptake rate, would reduce, at least partially, the depressing effect of the acid concentration [26]. This statement will hold better for “hot” plasma conditions. Under these conditions the interference is likely to be mainly due to the sample introduction system. This way, as a peristaltic pump allows the sample uptake rate to be kept constant, the decrease in the analyte transport rate should be smaller, and the same should happen for the interference degree. Under “cold” conditions the overall situation would be somewhat more complex, since the effects due to the plasma are higher. Using a peristaltic pump will cause simultaneous increases in both analyte and solvent (i.e., acid) transport rates, making the final overall effect to be unpredictable. Anyway, it could be expected that using a peristaltic pump under condition 1 should reduce the interference degree to a higher extent than under condition 3. This behaviour has also been observed in our case (Fig. 1d). From a comparison of Figs 1c and 1d, it appears that the behaviour is similar in both sample uptake modes but the emission intensity reductions are smaller in controlled uptake mode. Thus, for the highest acid concentration the decrease reaches 40–50% for the first group of acids, and 50–60% for the second (Fig. 1d). Another significant difference between the two sample uptake modes is that, under controlled uptake mode, the behaviour of H<sub>3</sub>PO<sub>4</sub> approaches that of the first group of acids.

From these results it can be concluded that, under our conditions, the interference appears to be similar for atomic and ionic lines, and independent of the energy of the line. In addition, the degree of the interference in controlled uptake mode is lower than in natural uptake mode. All these facts can be explained because of using “hot” plasma conditions. Again, the results shown in Fig. 1d agree with those obtained by some authors [34] and disagree with others [28]. This would mean that, under the conditions used for obtaining the signal, the main contribution to the acid interference is due to the sample introduction system.

## B. Discussion of the causes of the acid interference

As indicated in the Introduction, the contributions to the acid interference can be divided into two classes: (a) those arising from the sample introduction system; and (b) those originated into the plasma. The first ones will always appear, while the extent of the second ones will be dependent on the instrumental conditions (i.e., incident power, carrier gas flow and type and energy of the emission line).

The second part of the work is devoted to study the extent of each of the contribution classes. The contributions due to the sample introduction system are treated in sections B.1 to B.3 and those due to the plasma in section B.4.

**B.1. Changes in the sample uptake rate due to changes in the sample physical properties.** Table 3 shows some of the most significant physical properties of the solutions studied. Figure 2 shows the sample uptake rate values, under free aspiration (i.e., natural uptake rate,  $Q_n$ ), for the acids and concentrations studied. On comparing

Table 3. Physical properties of the solutions\*

% acid	Solution (w/w)	Relative viscosity†	Density‡ (kg/l)
0	HCl	1.000	0.9982
0.5	HCl	1.006	1.0007
5	HCl	1.073	1.0228
30	HCl	1.702	1.1492
0	HNO <sub>3</sub>	1.000	0.9982
0.5	HNO <sub>3</sub>	1.002	1.0009
5	HNO <sub>3</sub>	1.016	1.0257
30	HNO <sub>3</sub>	1.308	1.1801
0	HClO <sub>4</sub>	1.000	0.9982
0.5	HClO <sub>4</sub>	0.916	1.0028
5	HClO <sub>4</sub>	0.935	1.0280
30	HClO <sub>4</sub>	1.170	1.2067
0	H <sub>2</sub> SO <sub>4</sub>	1.000	0.9982
0.5	H <sub>2</sub> SO <sub>4</sub>	1.008	1.0016
5	H <sub>2</sub> SO <sub>4</sub>	1.110	1.0318
30	H <sub>2</sub> SO <sub>4</sub>	1.997	1.2191
0	H <sub>3</sub> PO <sub>4</sub>	1.000	0.9982
0.5	H <sub>3</sub> PO <sub>4</sub>	1.008	1.0010
5	H <sub>3</sub> PO <sub>4</sub>	1.136	1.0254
30	H <sub>3</sub> PO <sub>4</sub>	2.548	1.1804

\* Physical properties of HClO<sub>4</sub> solutions were obtained experimentally and all the other data from *CRC Handbook of Chemistry and Physics*, Ed. R. C. Weast, 70th Edn., CRC Press, Inc.(1989).

† Relative viscosity,  $\eta/\eta_0$ : Relation between the absolute viscosity of the solution at 20°C and the absolute viscosity of water at 20°C.

‡ At 20°C.

the data from Table 3 and Fig. 2, a clear correlation appears between natural uptake rate and solution viscosity (i.e.,  $Q_n$  decreases as solution viscosity increases). These data agree with the Volume Concentration (V.C.) values in Table 4A (natural uptake mode). The last column in Table 7A shows that the ratio  $I_{rel}/Q_n$  does not completely correct the interference. These results differ from those reported by other authors [16, 20,21] (under controlled uptake mode the values of this ratio are equal to those of  $I_{rel}$ ). Hence, the changes in  $Q_n$  would explain the differences in emission intensity between natural uptake mode and controlled uptake mode, but an additional explanation is needed to justify the intensity decreases observed under controlled uptake mode (Fig. 1d).

#### B.2. Changes in drop size distributions of the aerosols due to changes in the sample physical properties.

B.2.1. Primary aerosol. The NUKIYAMA-TANASAWA equation has been used for more than 50 years to predict the Sauter mean diameter of the aerosols generated pneumatically, under a given set of experimental conditions, as a function of the physical properties of the solution (i.e., density, viscosity and surface tension) [37]. Recently, it has been shown that such an equation does not predict accurately either the absolute values or the trends of the Sauter mean diameters [38, 39]. However, it is clear that there is a relationship between this statistical diameter and the physical properties of the solution, mainly surface tension and viscosity. To our knowledge, this is the first time that drop size distributions of the primary aerosols generated from solutions of increasing acid concentration are measured.

Table 4 shows some of the most significant parameters of the drop size distribution of the primary aerosols obtained, both in natural and controlled uptake modes, with all the acids under study. It is certainly striking that the values for the 0% solutions

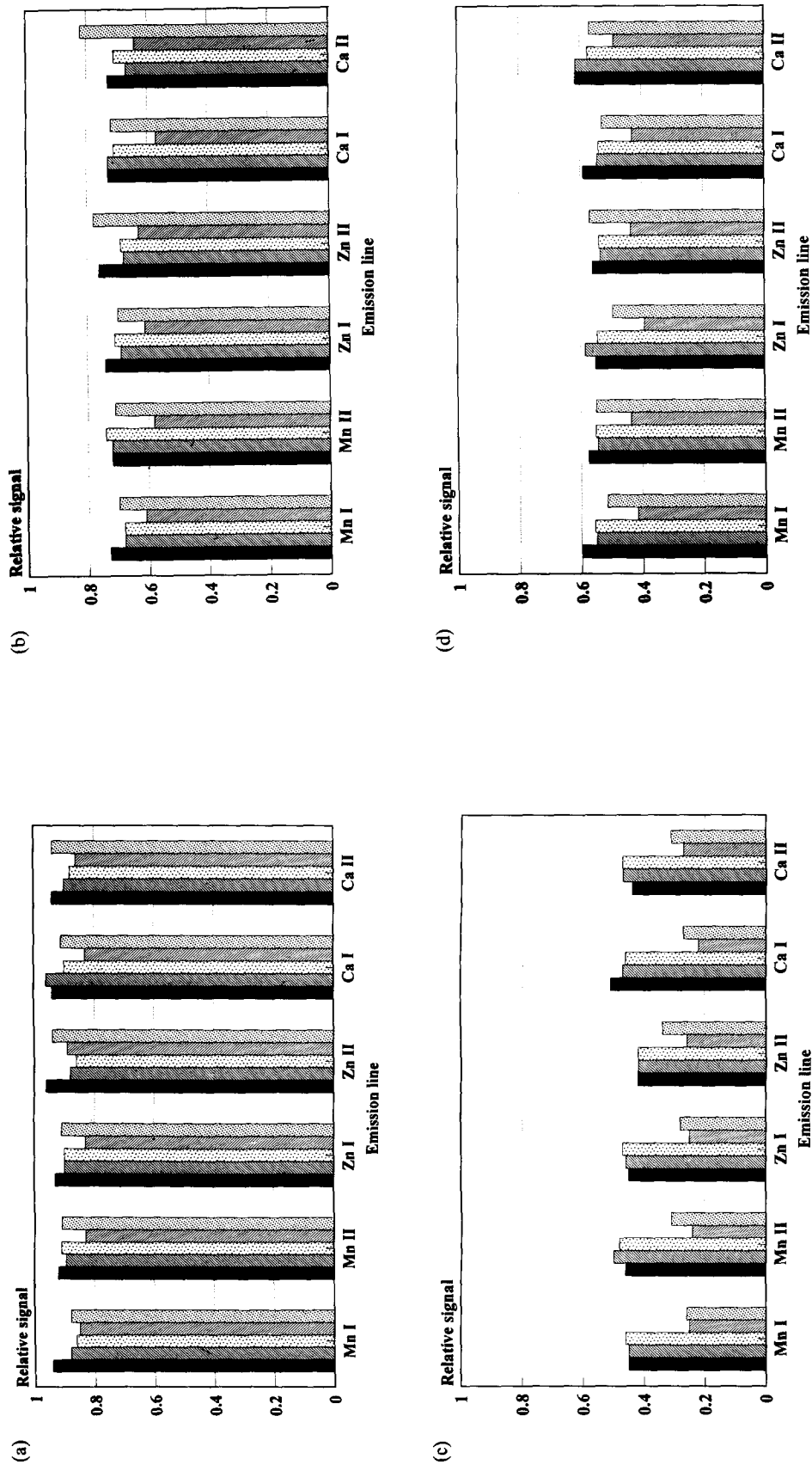


Fig. 1. Variation of relative emission intensity for all the elements and lines studied vs. acid concentration. Sample uptake mode: Natural (a, b and c); and controlled (d). Acid concentration, % (w/w): 0.5 (a); 5 (b); and 30 (c and d). Acid: ■ HCl, ▨ HNO<sub>3</sub>, ▩ H<sub>2</sub>SO<sub>4</sub>, ▪ HClO<sub>4</sub>, ▫ H<sub>3</sub>PO<sub>4</sub>.

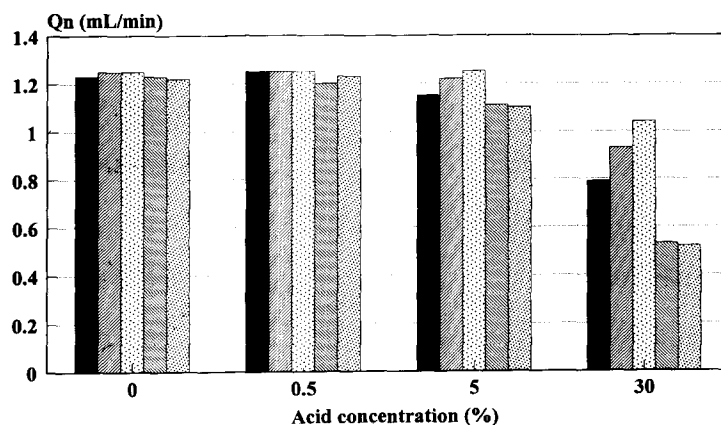


Fig. 2. Variation of the natural uptake rate,  $Q_n$ , vs. acid concentration.

Acid: ■ HCl ▨ HNO<sub>3</sub> ▤ HClO<sub>4</sub> ▩ H<sub>2</sub>SO<sub>4</sub> ▪ H<sub>3</sub>PO<sub>4</sub>

do not usually coincide among different series. However, it has been observed that the precision is higher within a series than between series. Several measurements were repeated to confirm these results. A satisfactory explanation to these discrepancies has not been found but certainly they are related with the measurement of the background, that is performed at the beginning of each series. The precision of the measurements within a series validate the trends observed. From the results, it arises that, under natural uptake mode, as HCl concentration increases primary aerosol becomes finer, while under controlled aspiration it becomes slightly coarser. With H<sub>2</sub>SO<sub>4</sub> solutions, in natural uptake mode, the drop size distribution firstly shows a slight increase, and then decreases for the highest H<sub>2</sub>SO<sub>4</sub> concentration. In controlled uptake mode the mean drop size of the distributions increase noticeably on increasing H<sub>2</sub>SO<sub>4</sub> concentration, mainly at 30%. Figure 3 shows the primary drop size distributions of the aerosols generated in controlled uptake mode with solutions of different H<sub>2</sub>SO<sub>4</sub> concentration. It appears that the shape of the distribution changes on increasing the acid concentration, these changes being more noticeable for drop sizes over 30  $\mu\text{m}$ . Because of this, for the 0% acid concentration solution about 100% of the aerosol volume is contained in droplets smaller than 60  $\mu\text{m}$ , whereas for the 30% solution the aerosol volume contained in droplets larger than 60  $\mu\text{m}$  is not negligible. From these results, it could be anticipated that, under controlled uptake mode, the volume of aerosol, and hence, the analyte mass, lost in the spray chamber will increase on increasing the acid concentration.

From the data shown up to now, it can be concluded that solution physical properties play an important double role. Firstly, they modify the natural uptake rate, as has been shown in the previous section (Fig. 2). Secondly, they determine the characteristics of the primary aerosols. Once again two behaviours can be observed. On one hand, on increasing HCl, HNO<sub>3</sub> and HClO<sub>4</sub> concentration, the primary aerosols become slightly finer in natural uptake mode, while under controlled uptake mode, they do not change or even become slightly coarser. In order to try to explain this behaviour one should bear in mind the microscopic mechanism of aerosol pneumatic generation. Surface is generated by means of energy transfer from a high velocity gas stream to a liquid stream. In natural uptake mode, an increase in acid concentration makes liquid flow decrease. Hence, for a constant nebulizing gas flow, there is a higher amount of kinetic energy per unit of liquid volume. This leads to the generation of a finer aerosol. In controlled aspiration mode, for the same group of acids, the kinetic energy to liquid volume ratio is always the same, and hence, the effect of the physical properties is not counterbalanced by a higher kinetic energy to liquid volume ratio. Therefore, a slightly coarser aerosol should be obtained. On the other hand, for H<sub>2</sub>SO<sub>4</sub> and H<sub>3</sub>PO<sub>4</sub>, in natural uptake mode, the increase in viscosity is counterbalanced by a decrease in  $Q_n$ , showing the median and mass mean diameters of the primary



Table 4. Parameters of primary drop size distributions

% acid	Solution (w/w)	$D_{4,3}^*$ ( $\mu\text{m}$ )	$D_{50}^\dagger$ ( $\mu\text{m}$ )	Span $^\ddagger$	V.C. $\times 10^4$ $^\S$ (%)
A. Natural uptake mode					
0	HCl	14.90	11.90	2.59	6
0.5	HCl	14.94	11.93	2.59	6
5	HCl	14.84	11.86	2.58	5
30	HCl	13.65	11.22	2.47	4
0	HNO <sub>3</sub>	15.02	11.88	2.62	6
0.5	HNO <sub>3</sub>	14.89	11.83	2.61	6
5	HNO <sub>3</sub>	14.99	11.82	2.64	6
30	HNO <sub>3</sub>	13.79	11.09	2.54	5
0	HClO <sub>4</sub>	14.97	11.87	2.61	6
0.5	HClO <sub>4</sub>	15.16	11.93	2.65	6
5	HClO <sub>4</sub>	15.09	11.82	2.68	6
30	HClO <sub>4</sub>	13.78	11.03	2.57	5
0	H <sub>2</sub> SO <sub>4</sub>	14.40	11.82	2.45	6
0.5	H <sub>2</sub> SO <sub>4</sub>	14.56	11.81	2.49	6
5	H <sub>2</sub> SO <sub>4</sub>	14.51	11.70	2.51	5
30	H <sub>2</sub> SO <sub>4</sub>	13.99	11.49	2.37	2
0	H <sub>3</sub> PO <sub>4</sub>	13.98	11.34	2.53	5
0.5	H <sub>3</sub> PO <sub>4</sub>	14.14	11.46	2.53	5
5	H <sub>3</sub> PO <sub>4</sub>	14.28	11.57	2.54	5
30	H <sub>3</sub> PO <sub>4</sub>	13.80	11.25	2.52	2
B. Controlled uptake mode ( $Q_1 = 1$ ml/min)					
0	HCl	15.09	12.10	2.51	4
0.5	HCl	15.14	12.08	2.55	4
5	HCl	15.32	12.16	2.56	4
30	HCl	16.24	12.52	2.72	5
0	HNO <sub>3</sub>	14.67	11.78	2.47	4
0.5	HNO <sub>3</sub>	14.77	11.80	2.52	4
5	HNO <sub>3</sub>	15.12	11.97	2.56	4
30	HNO <sub>3</sub>	15.10	11.82	2.64	5
0	HClO <sub>4</sub>	14.61	11.73	2.48	4
0.5	HClO <sub>4</sub>	14.76	11.78	2.51	4
5	HClO <sub>4</sub>	14.43	11.69	2.42	4
30	HClO <sub>4</sub>	14.88	11.46	2.75	5
0	H <sub>2</sub> SO <sub>4</sub>	13.94	11.18	2.46	4
0.5	H <sub>2</sub> SO <sub>4</sub>	13.89	11.08	2.49	4
5	H <sub>2</sub> SO <sub>4</sub>	14.17	11.19	2.55	4
30	H <sub>2</sub> SO <sub>4</sub>	18.21	13.10	2.96	5
0	H <sub>3</sub> PO <sub>4</sub>	14.04	11.36	2.42	4
0.5	H <sub>3</sub> PO <sub>4</sub>	14.33	11.44	2.51	4
5	H <sub>3</sub> PO <sub>4</sub>	14.58	11.56	2.56	4
30	H <sub>3</sub> PO <sub>4</sub>	19.98	14.19	2.89	5

\*  $D_{4,3}$ : Mean diameter of the volume (mass) distribution.

†  $D_{50}$ : Median of the volume (mass) distribution.

‡ Span: Measure of the distribution dispersion in terms of  $D_{50}$ .

§ Volume concentration, V.C.: Percentile of the active volume (a cylinder of 14.5 mm long and 9 mm diameter) occupied by liquid droplets.

drop size distribution a slight maximum as the acid concentration increases. However, in controlled mode the sample physical properties dominate the aerosol generation process, always giving rise to coarser aerosols.

B.2.2. Tertiary aerosol. The more outstanding aspects of the few papers dealing with the measurement of the drop size distributions (or dry particle distributions) of the tertiary aerosols generated from acid solutions have been discussed extensively in

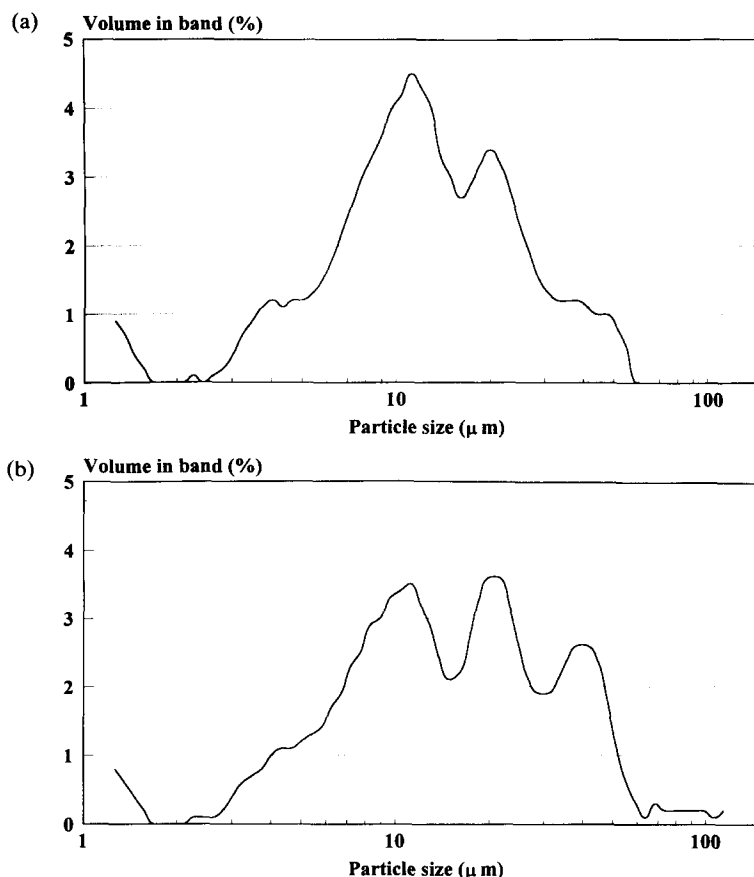


Fig. 3. Drop size distribution of primary aerosols generated with solutions of different  $\text{H}_2\text{SO}_4$  concentration. Sample uptake mode: Controlled. Acid concentration, % (w/w): 0 (a) and 30 (b). Distribution in volume (mass) frequency.

the Introduction [17, 18, 25]. In all these papers, the aerosols have been characterized by means of optical methods.

Table 5 shows the most significant parameters of the tertiary drop size distributions of the aerosols obtained with all the acids and concentrations studied. From these data it appears that statistical and characteristic diameters decrease on increasing acid concentration. These results differ from those of CLIFFORD *et al.* [18], but agree with those of KITAGAWA and KIKUCHI [17], and MARICHY *et al.* [25]. At low acid concentrations, the tertiary aerosol shows little variation, while at high concentrations it becomes finer and more disperse (i.e., its Span value increases). The differences with the data provided by CLIFFORD *et al.* [18] could be due to two possible causes: (a) these authors make use of a different nebulizer, which is coupled to a desolvation unit, and, hence, the mechanisms of aerosol generation and transport are different; and (b) the laser-diffraction (Malvern) instrument used in this work measures a line-of-sight average through the complete spray; that is, it samples drops within the volume defined by the intersection of the laser beam and the spray; the phase/Doppler (Aerometrics) used by CLIFFORD *et al.* [18], on the other hand, samples in a very small volume rather than through the whole spray [40]. In order to explain these behaviours a density-effect may be considered when the acid concentration increases. The probability for a droplet to exit the spray chamber decreases on increasing the solution density. Two droplets of the same size but with different densities will have different inertias (different weights), and, hence, the droplet with higher density will have a smaller probability of exiting the spray chamber. This density-effect would be equivalent to a reduction in the cut-off diameter of the spray chamber. Therefore, the higher the

Table 5. Parameters of the tertiary drop size distributions

% acid	Solution (w/w)	$D_{4.3}$ ( $\mu\text{m}$ )	$D_{50}$ ( $\mu\text{m}$ )	Span	V.C. $\times 10^4$ (%)
A. Natural uptake mode					
0	HCl	5.35	4.46	2.34	1
0.5	HCl	5.07	4.17	2.46	1
5	HCl	4.75	3.91	2.47	1
30	HCl	4.36	3.48	2.50	2
0	HNO <sub>3</sub>	5.04	4.21	2.40	1
0.5	HNO <sub>3</sub>	5.00	4.12	2.48	1
5	HNO <sub>3</sub>	4.93	4.00	2.57	2
30	HNO <sub>3</sub>	4.37	3.47	2.66	2
0	HClO <sub>4</sub>	5.08	4.24	2.41	1
0.5	HClO <sub>4</sub>	5.01	4.13	2.50	1
5	HClO <sub>4</sub>	4.63	3.74	2.64	1
30	HClO <sub>4</sub>	4.19	3.37	2.71	2
0	H <sub>2</sub> SO <sub>4</sub>	5.38	4.49	2.36	1
0.5	H <sub>2</sub> SO <sub>4</sub>	5.13	4.23	2.47	1
5	H <sub>2</sub> SO <sub>4</sub>	4.66	3.79	2.59	1
30	H <sub>2</sub> SO <sub>4</sub>	3.80	3.13	2.59	1
0	H <sub>3</sub> PO <sub>4</sub>	5.60	4.67	2.34	1
0.5	H <sub>3</sub> PO <sub>4</sub>	5.29	4.39	2.40	1
5	H <sub>3</sub> PO <sub>4</sub>	4.78	3.91	2.55	1
30	H <sub>3</sub> PO <sub>4</sub>	3.79	3.11	2.62	1
B. Controlled uptake mode ( $Q_1 = 1$ ml/min)					
0	HCl	5.60	4.60	2.46	1
0.5	HCl	5.30	4.29	2.56	1
5	HCl	5.24	4.20	2.59	2
30	HCl	4.60	3.53	2.69	2
0	HNO <sub>3</sub>	5.79	4.72	2.35	1
0.5	HNO <sub>3</sub>	5.06	4.14	2.52	1
5	HNO <sub>3</sub>	4.86	3.89	2.67	2
30	HNO <sub>3</sub>	4.43	3.55	2.64	2
0	HClO <sub>4</sub>	5.16	4.21	2.58	1
0.5	HClO <sub>4</sub>	4.86	3.95	2.63	1
5	HClO <sub>4</sub>	4.65	3.72	2.70	2
30	HClO <sub>4</sub>	3.89	3.14	2.72	2
0	H <sub>2</sub> SO <sub>4</sub>	5.39	4.48	2.40	1
0.5	H <sub>2</sub> SO <sub>4</sub>	5.25	4.31	2.51	1
5	H <sub>2</sub> SO <sub>4</sub>	4.72	3.82	2.62	1
30	H <sub>2</sub> SO <sub>4</sub>	4.27	3.50	2.60	1
0	H <sub>3</sub> PO <sub>4</sub>	5.51	4.61	2.36	1
0.5	H <sub>3</sub> PO <sub>4</sub>	5.44	4.49	2.44	1
5	H <sub>3</sub> PO <sub>4</sub>	5.00	4.05	2.59	1
30	H <sub>3</sub> PO <sub>4</sub>	4.24	3.46	2.63	1

solution density, the finer the tertiary aerosol. In addition, the amount of tertiary aerosol would also decrease on increasing the solution density.

**B.3. Changes in total analyte transport rate due to changes in sample uptake rate and/or in the drop size distribution.** As was indicated in the Introduction, few papers have been published that include data about analyte and/or solution transport, and these data appear to be, again, partial and contradictory [17, 18, 20, 24, 25].

From the results shown up to here, it can be expected that the analyte transport should decrease, under natural uptake mode, because of the decrease on  $Q_n$ , while under controlled uptake mode because of the larger size of the primary aerosol. Both effects are originated by the increased viscosity. The effect of the increased density

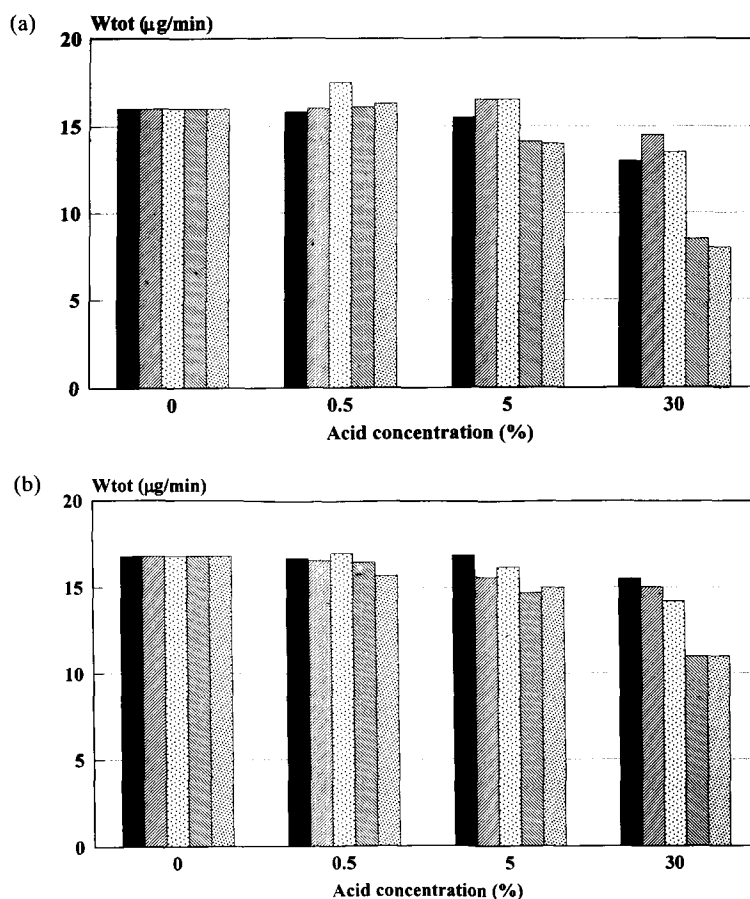


Fig. 4. Variation of total analyte transport rate,  $W_{\text{tot}}$ , vs. acid concentration. Analyte: Mn. Sample uptake mode: Natural (a); and controlled (b). Acid: ■ HCl ▨ HNO<sub>3</sub> ▤ HClO<sub>4</sub> ▩ H<sub>2</sub>SO<sub>4</sub> ▪ H<sub>3</sub>PO<sub>4</sub>

would also cause a decrease in the transport. Moreover, as a consequence of their higher viscosity, the acids of the second group (i.e., H<sub>2</sub>SO<sub>4</sub> and H<sub>3</sub>PO<sub>4</sub>) undergo the greatest variations in  $Q_n$ , under natural uptake mode, and in the primary drop size distributions, under controlled uptake mode. Hence, these acids can be expected to show the greatest variations in  $W_{\text{tot}}$ , under both sample uptake modes.

Figure 4 shows the total analyte (Mn) transport rate to the plasma,  $W_{\text{tot}}$ , versus acid concentration, under both natural (Fig. 4a) and controlled (Fig. 4b) uptake modes. In order to explain these data one should take into account the results shown in Tables 4 and 5 and Fig. 2. For the first group of acids (i.e., HCl, HNO<sub>3</sub> and HClO<sub>4</sub>), in controlled uptake mode,  $W_{\text{tot}}$  values are almost constant, showing a slight decrease for the highest value of the acid concentration (30%). This agrees with the distribution data for the primary (Table 4B) and tertiary (Table 5B) aerosols. In this case, an additional small amount of analyte will be lost due to the increasing density of the solutions. For the same group of acids, under natural uptake mode, there are two opposite effects. On increasing acid concentration, on one side, primary aerosols are slightly finer (Table 4A), while, on the other side, the natural uptake rate decreases (Fig. 2). The final result is that the  $W_{\text{tot}}$  values do show a decrease, but smaller than if the primary aerosol would have been coarser.

With the second group of acids (i.e., H<sub>2</sub>SO<sub>4</sub> and H<sub>3</sub>PO<sub>4</sub>), the physical properties of the solutions play a more significant role. Thus, in natural uptake mode they reduce noticeably the aspiration rate (Fig. 2), while in controlled mode they increase the drop size distribution of the primary aerosol (Table 4B). However, under controlled uptake mode the sample uptake rate is constant, while in natural mode the primary drop size

Table 6. Relative analyte transport rate

Solution		$(W_{\text{tot}})_{\text{rel}}^*$	
% acid	(w/w)	Natural uptake mode	Controlled uptake mode
0	HCl	0.99	1.01
0.5	HCl	—	—
5	HCl	—	—
30	HCl	0.96	0.97
0	HNO <sub>3</sub>	0.99	1.01
0.5	HNO <sub>3</sub>	1.02	0.99
5	HNO <sub>3</sub>	1.02	0.96
30	HNO <sub>3</sub>	0.99	1.00
0	HClO <sub>4</sub>	0.99	1.01
0.5	HClO <sub>4</sub>	0.99	0.99
5	HClO <sub>4</sub>	0.99	1.04
30	HClO <sub>4</sub>	1.02	1.01
0	H <sub>2</sub> SO <sub>4</sub>	0.99	1.01
0.5	H <sub>2</sub> SO <sub>4</sub>	1.01	1.00
5	H <sub>2</sub> SO <sub>4</sub>	1.01	1.00
30	H <sub>2</sub> SO <sub>4</sub>	0.95	0.99
0	H <sub>3</sub> PO <sub>4</sub>	0.99	1.01
0.5	H <sub>3</sub> PO <sub>4</sub>	1.00	1.00
5	H <sub>3</sub> PO <sub>4</sub>	0.99	0.99
30	H <sub>3</sub> PO <sub>4</sub>	0.99	1.03

$$* (W_{\text{tot}})_{\text{rel}} = (W_{\text{tot}})_{\text{Zn}} / (W_{\text{tot}})_{\text{Mn}}$$

distributions are slightly reduced. Hence, the combination of these effects causes transport to decrease significantly, to a greater extent in natural uptake mode (Fig. 4a). Taking into account the experimental error of these measurements, one can say that the decreases in  $W_{\text{tot}}$  appear clearly just for the highest concentrations, 30% for the first group of acids and 5% for those of the second one. These results seem not to agree with the data reported by other authors [18, 25]. However, the comparison is not straightforward. Thus, MARICHY *et al.* [25] measured the transport of solvent in solutions of low HCl concentration. CLIFFORD *et al.* [18] used a sample introduction system very different to ours, and, in addition, they were not very confident on their own conclusions because of instrumental limitations. These limitations had been previously reported by DODGE *et al.* [40].

From all these data it can be concluded that in natural uptake mode the variations in  $W_{\text{tot}}$  values are dependent on the sample aspiration rate, while in controlled uptake mode these variations are dependent on the primary drop size distribution. The data of transport at high acid concentration (30%) allow us to explain why the interference degree in controlled uptake mode is lower than in natural uptake mode, and also lower for the first group of acids than for the second.

If the density-effect described above is considered it would influence analyte transport in the same direction as has been previously discussed for drop size distribution and  $Q_n$ .

Table 6 shows that  $W_{\text{tot}}$  values are similar for Mn and Zn, and this means a similar behaviour for both analytes during aspiration, nebulization and transport. If the behaviours of both analytes are also similar in the plasma, the internal standard method could be applied in order to correct the acid interference [24, 29–32].

**B.4. Changes in the plasma excitation conditions due to the increased energy consumption for the acid atomization.** The variations in analyte transport rate can be useful to explain the interference caused by the mineral acids. However, an additional effect should be taken into consideration in order to account for the interference with the first group of acids, since analyte transport remains almost constant (Fig. 4b) up to 30% acid concentration, under controlled uptake mode, and up to 5% in natural

Table 7. Variations of signal to transport and signal to natural uptake rate ratios

% acid	Solution (w/w)	Analyte and type of line	$I_{rel}$	$(I_{rel}/W_{tot})_n$	$(I_{rel}/Q_n)_n$
A. Natural uptake mode					
0	HCl	Mn I	1.00	1.00	1.00
0.5	HCl	Mn I	0.94	0.95	0.94
5	HCl	Mn I	0.73	0.75	0.79
30	HCl	Mn I	0.45	0.55	0.73
0	HCl	Mn II	1.00	1.00	1.00
0.5	HCl	Mn II	0.92	0.93	0.92
5	HCl	Mn II	0.72	0.74	0.77
30	HCl	Mn II	0.46	0.57	0.74
0	H <sub>2</sub> SO <sub>4</sub>	Mn I	1.00	1.00	1.00
0.5	H <sub>2</sub> SO <sub>4</sub>	Mn I	0.85	0.84	0.87
5	H <sub>2</sub> SO <sub>4</sub>	Mn I	0.61	0.69	0.69
30	H <sub>2</sub> SO <sub>4</sub>	Mn I	0.25	0.47	0.58
0	H <sub>2</sub> SO <sub>4</sub>	Mn II	1.00	1.00	1.00
0.5	H <sub>2</sub> SO <sub>4</sub>	Mn II	0.83	0.83	0.85
5	H <sub>2</sub> SO <sub>4</sub>	Mn II	0.58	0.66	0.65
30	H <sub>2</sub> SO <sub>4</sub>	Mn II	0.24	0.45	0.57
B. Controlled uptake mode ( $Q_1 = 1$ ml/min)					
0	HCl	Mn I	1.00	1.00	
0.5	HCl	Mn I	0.94	0.95	
5	HCl	Mn I	0.76	0.75	
30	HCl	Mn I	0.60	0.65	
0	HCl	Mn II	1.00	1.00	
0.5	HCl	Mn II	0.93	0.94	
5	HCl	Mn II	0.75	0.75	
30	HCl	Mn II	0.58	0.62	
0	H <sub>2</sub> SO <sub>4</sub>	Mn I	1.00	1.00	
0.5	H <sub>2</sub> SO <sub>4</sub>	Mn I	0.91	0.93	
5	H <sub>2</sub> SO <sub>4</sub>	Mn I	0.66	0.75	
30	H <sub>2</sub> SO <sub>4</sub>	Mn I	0.42	0.63	
0	H <sub>2</sub> SO <sub>4</sub>	Mn II	1.00	1.00	
0.5	H <sub>2</sub> SO <sub>4</sub>	Mn II	0.92	0.93	
5	H <sub>2</sub> SO <sub>4</sub>	Mn II	0.71	0.81	
30	H <sub>2</sub> SO <sub>4</sub>	Mn II	0.44	0.66	

uptake mode (Fig. 4a). Hence, this additional effect should be originated in the plasma itself. If the interference would have been produced exclusively during the generation and/or transport of the aerosol, it would have been possible to compensate it for by means of the ratios  $I_{rel}/Q_n$  [16] or  $I_{rel}/W_{tot}$  [20].

Table 7 shows the variations of signal to transport ratio,  $(I_{rel}/W_{tot})_n$ , and signal to natural uptake rate ratio,  $(I_{rel}/Q_n)_n$ , for two acids, one of each group. From these data it appears that these ratios decrease on increasing acid concentration. The reduction in the signal to transport ratio is indicating a loss of efficiency in the production of analytical signal. This loss of efficiency in the production of analytical signal may be attributed to two possible causes: (i) tertiary aerosol is getting coarser or; (ii) the energy consumption to atomize the increasing amount of acid is getting higher, thus causing a plasma cooling. The former can be discarded from the data shown in Table 5, where the tertiary aerosol becomes finer on increasing acid concentration. Hence, the only possibility is the second one. Figure 5 shows the excitation temperature variations with acid concentration under natural (Fig. 5a) and controlled (Fig. 5b) uptake modes. A systematic and reproducible drop in excitation temperature is observed for all the acids at high concentrations, this drop being specially pronounced for H<sub>2</sub>SO<sub>4</sub>. The fact that  $T_{exc}$  does not change with acid

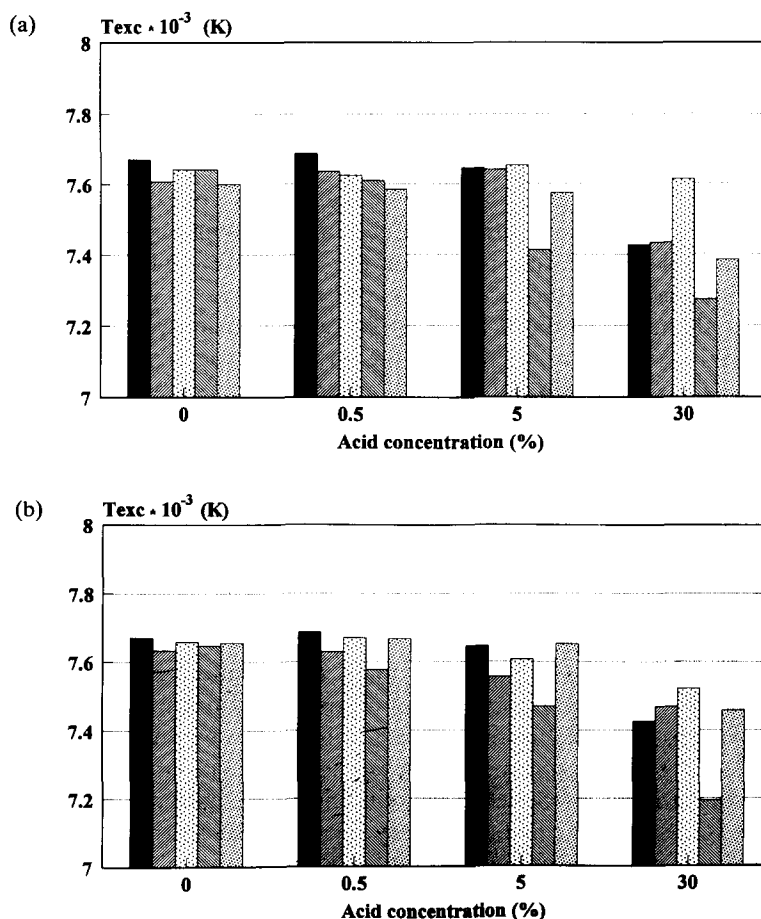


Fig. 5. Variation of plasma excitation temperature vs. acid concentration. Sample uptake mode: Natural (a); and controlled (b). Acid: ■ HCl ▨ HNO<sub>3</sub> ▩ HClO<sub>4</sub> ▤ H<sub>2</sub>SO<sub>4</sub> ▦ H<sub>3</sub>PO<sub>4</sub>

concentration, at low concentrations, agrees with the results reported by some authors [15, 34] and differs from others [28].

For the first group of acids, the variations in  $W_{tot}$  and  $T_{exc}$  values, at low acid concentrations ( $< 5\%$ ), are so small that they can hardly explain the extent of the interference. This would mean that there is, at least, some other parameter of plasma, not measured in our case, that is influenced by the presence of the acids, or, alternatively, that the lack of precision in the  $W_{tot}$  and  $T_{exc}$  measurements do not allow the detection of small changes in these magnitudes.

## CONCLUSIONS

The results obtained in the present work have allowed us to confirm some previous results and to discard some others. At the same time new results have been reported that are essential for a better understanding of the interfering effect of the mineral acids in atomic spectrometry.

The previously established conclusions that, under our conditions, have been confirmed would be: 1. The physical properties of the acid solutions are in the origin of the interference of mineral acids in ICP-AES. The changes in the physical properties of the solutions are reflected with different intensity depending on the acid nature and mode of the sample introduction (i.e., natural or controlled).

2. The interference effect of mineral acids in ICP-AES is contributed by several factors: sample uptake rate, drop size distributions, transport rates and plasma

excitation conditions. The first three factors arise from changes in the physical properties of the solutions.

3. From the point of view of the degree of interference, the mineral acids studied can be classified in two groups, HCl, HNO<sub>3</sub> and HClO<sub>4</sub> in the first one, and H<sub>2</sub>SO<sub>4</sub> and H<sub>3</sub>PO<sub>4</sub> in the second one. This behaviour is in agreement with the viscosity of the solutions.

4. In both uptake modes a cooling effect of the plasma could exist, depending on the instrumental conditions, due to the presence of increasing amounts of acids.

The conclusions reported in this paper for the first time would be: 5. In natural uptake mode an increase in acid concentration causes a decrease in the natural sample uptake rate and a slight reduction of the drop size of the primary aerosol. The overall contribution of these contradictory factors tends to reduce the  $W_{\text{tot}}$  values and, hence, the emission signal. So, in natural uptake mode the contribution of the sample introduction system to the interference effect of mineral acids is dominated mainly by the sample uptake rate.

6. In controlled uptake mode an increase in acid concentration increases the primary drop size distribution of the aerosols, while sample uptake rate does not change. The combined effect of both circumstances produces a decrease in  $W_{\text{tot}}$  values and, hence, in emission signal. So, in controlled uptake mode the contribution of the sample introduction system to the interference effect of mineral acids depends mainly on the primary drop size distribution.

7. In addition, a density-effect may contribute to the interference, decreasing the amount of sample reaching the plasma on increasing acid concentration.

Finally, some suggestions for future work could be: 8. To extend this kind of studies to other nebulizers (e.g., thermospray, ultrasonic, . . .), in order to elucidate the contributions of the sample introduction system and of the plasma itself.

9. To perform similar studies at low or very low acid concentrations (< 5%, w/w), in order to check the possible existence of an AIR [25].

10. To check the possibility of correcting this interference, in a general way. One can expect that using, simultaneously, a controlled uptake system, an internal standard and "hot" plasma conditions would reduce or even eliminate this interference.

**Acknowledgements**—The authors thank the DGICYT (Spain) for financial support of the present study (Project: PB92-0336) and BAIRD Corporation for facilitating the plasma spectrometer purchase. A.C. wishes to express his appreciation to the Consellería de Cultura, Educación y Ciencia de la Generalidad Valenciana (Spain) for scholarship. Valuable comments and suggestions provided by the reviewers are gratefully acknowledged.

## REFERENCES

- [1] J. Sneddon (Ed.), *Sample Introduction in Atomic Spectroscopy*. Elsevier Science Publishers B.V., Amsterdam (1990).
- [2] R. F. Browner, in *Inductively Coupled Plasma Emission Spectroscopy. Part II: Applications and Fundamentals*, Ed. P. W. J. M. Boumans, p. 244. John Wiley & Sons, New York (1987).
- [3] A. G. T. Gustavsson, in *Inductively Coupled Plasmas in Analytical Atomic Spectrometry*, Eds. A. Montaser and D. W. Golightly, p. 399. VCH Publishers, Inc., New York (1987).
- [4] J. L. M. de Boer and F. J. M. J. Maessen, *Spectrochim. Acta* **38B**, 739 (1983).
- [5] A. López-Molinero, J. R. Castillo and A. De Vega, *Fresenius Z. Anal. Chem.* **331**, 721 (1988).
- [6] K. A. Wolnik, R. W. Kuennen and F. L. Fricke, in *Developments in Atomic Plasma Spectrochemical Analysis*, Ed. R. M. Barnes, p. 685. Heyden, London (1981).
- [7] S. E. Church, in *Developments in Atomic Plasma Spectrochemical Analysis*, Ed. R. M. Barnes, p. 410. Heyden, London (1981).
- [8] R. C. Munter and R. A. Grande, in *Developments in Atomic Plasma Spectrochemical Analysis*, Ed. R. M. Barnes, p. 653. Heyden, London (1981).
- [9] H. M. Kingston and L. B. Jassie (Eds), *Introduction to Microwave Sample Preparation. Theory and Practice*. ACS, Washington DC (1988).
- [10] M. Thompson, in *Inductively Coupled Plasmas in Analytical Atomic Spectrometry*, Eds A. Montaser and D. W. Golightly, p. 185. VCH Publishers, Inc., New York (1987).
- [11] P. Schramel and J. Ovcár-Pavlu, *Fresenius Z. Anal. Chem.* **298**, 28 (1979).
- [12] M. T. C. de Loos-Vollebregt, R. Peng and J. J. Tigelman, *J. Anal. At. Spectrom.* **6**, 165 (1991).
- [13] S. S. Berman, J. W. McLaren and S. N. Willie, *Anal. Chem.* **52**, 488 (1980).



- [14] J. J. Zhu, *Elimination of Acid Matrix and Organic Solvent Interferences in Ultrasonic Nebulization ICP-AES*. Oral presentation #1266. The Pittsburgh Conference. Atlanta, GA (1993).
- [15] A. Fernández, M. Murillo, N. Carrión and J. M. Mermet, *J. Anal. At. Spectrom.* **9**, 217 (1994).
- [16] S. Greenfield, H. M. McGeachin and P. B. Smith, *Anal. Chim. Acta* **84**, 67 (1976).
- [17] K. Kitagawa and H. Kikuchi, *Anal. Sci.* **4**, 53 (1988).
- [18] R. H. Clifford, P. Sohal, H. Liu and A. Montaser, *Spectrochim. Acta* **47B**, 1107 (1992).
- [19] H. Kawaguchi, T. Ito, K. Ota and A. Mizuike, *Spectrochim. Acta* **35B**, 199 (1980).
- [20] J. Farino, J. R. Miller, D. D. Smith and R. F. Browner, *Anal. Chem.* **59**, 2303 (1987).
- [21] R. L. Dahlquist and J. W. Knoll, *Appl. Spectrosc.* **32**, 1 (1978).
- [22] H. Ishii and K. Satoh, *Talanta* **30**, 111 (1983).
- [23] M. A. E. Wandt, M. A. Bruno-Pouget and A. L. Rodgers, *Analyst* **109**, 1071 (1984).
- [24] X. E. Shen and Q. L. Chen, *Spectrochim. Acta* **38B**, 115 (1983).
- [25] M. Marichy, M. Mermet and J. M. Mermet, *Spectrochim. Acta* **45B**, 1195 (1990).
- [26] F. J. M. J. Maessen, J. Balke and J. L. M. De Boer, *Spectrochim. Acta* **37B**, 517 (1982).
- [27] E. G. Chudinov, I. I. Ostroukhova and G. V. Varvanina, *Fresenius Z. Anal. Chem.* **335**, 25 (1989).
- [28] E. Yoshimura, H. Suzuki, S. Yamazaki and S. Toda, *Analyst* **115**, 167 (1990).
- [29] L. M. Garden, J. Marshall and D. Littlejohn, *J. Anal. At. Spectrom.* **6**, 159 (1991).
- [30] R. K. Skogerboe and G. N. Coleman, *Appl. Spectrosc.* **30**, 504 (1976).
- [31] R. I. Botto, *Spectrochim. Acta* **40B**, 397 (1985).
- [32] P. J. McKinnon, K. C. Giess and T. V. Knight, in *Developments in Atomic Plasma Spectrochemical Analysis*, Ed. R. M. Barnes, p. 287. Heyden, London (1981).
- [33] A. Delijska and M. Vouchkov, *Fresenius Z. Anal. Chem.* **321**, 448 (1985).
- [34] B. Budic and V. Hudnik, *J. Anal. At. Spectrom.* **9**, 53 (1994).
- [35] J. M. Mermet, in *Inductively Coupled Plasma Emission Spectroscopy. Part II: Applications and Fundamentals*, Ed. P. W. J. M. Boumans, p. 353. John Wiley & Sons, New York (1987).
- [36] J. F. Alder, R. M. Bombelka and G. F. Kirkbright, *Spectrochim. Acta* **35B**, 163 (1980).
- [37] S. Nukiyama and Y. Tanasawa, *Trans. Soc. Mech. Eng. Jpn.* **5**, 68 (1939).
- [38] A. Canals, J. Wagner, R. F. Browner and V. Hernandis, *Spectrochim. Acta* **43B**, 1321 (1988).
- [39] A. Canals, V. Hernandis and R. F. Browner, *J. Anal. At. Spectrom.* **5**, 61 (1990).
- [40] L. G. Dodge, D. J. Rhodes and R. D. Reitz, *Appl. Opt.* **26**, 2144 (1987).